Diodicity mechanism Tesla-type microvalves: a CFD study

Wang, Liung and Xu, Lin and Tang, Yawen

Xi'an Jiaotong University, Xi'an, Shaanxi, China, Xi'an Jiaotong University, Xi'an, Shaanxi, China, Xi'an Jiaotong University, Xi'an, Shaanxi, China

16 March 2017

Diodicity mechanism Tesla-type microvalves: a CFD study

Liung Wang, Lin Xu, Yawen Tang

Xi’an Jiaotong University, Xi’an, Shaanxi, China

1. Abstract:

Microvalve is one of the most important components in microfluidic systems and micropumps. In this paper, three-dimensional incompressible flow through a Tesla-type microvalve is simulated using FLUENT computational fluid dynamic package. The flow is laminar and SIMPLE algorithm is used. The second-order upwind method is implemented for discretizing convective terms. The diodicity mechanism is investigated in detail for three different microvalves. Effect of several series Tesla-type microvalves on diodicity is also studied. The numerical analyses reveal that the mechanism of diodicity occurs at the T-junction and side channel. If inlet and outlet channels are eliminated, diodicity can be increased by 2. Pressure field analysis shows that the pressure drop is much severe at the junction of the reverse flow compared to the forward flow. The obtained numerical results are compared with those of experimental and a good agreement between them is noticed.

2. Introduction:

MEMS (Micro-Electro-Mechanical Systems) devices often contain microfluidic systems that are designed to move very small quantities of fluid, such as microliters or even nanoliters, within the device. A micropump is one of the main devices in this field, which can generate flow in the range of milliliters to microliters. Today, many potential applications for micropumps are still being investigated, involving in drug delivery, biological detection, clinical analysis in medicine, cardiology system, etc. Microvalves can be classified into active microvalves, using mechanical and nonmechanical moving parts, and passive microvalves, using mechanical and non-mechanical moving parts . Mechanical active microvalves employ the mechanically movable MEMS-based membranes which are coupled to magnetic , electric, piezoelectric actuation methods. The actuation principles of active microvalves with non-mechanical moving parts (NMP) are based on electrochemical , phase change , and rheological materials. Non-mechanical passive microvalves (fixed microvalves) involve no mechanical moving parts and provide the possibility to build the so-called valveless micropumps. Two main types of fixed microvalves have been used in valveless micro- pumps which are microdiffusers and Tesla microvalves .

Using of microvalves results in increased performance, efficiency, reliability and reduced size and cost of the equipments. The first microvalve was introduced by Terry in 1978 . The first commercial production started in 1990 and various types have been designed for different purposes up to now. One of the important applications of them is in heat control of electronic components at space equipments, such as micro-satellite . Calibration, testing, measurement of volumes in micro-scale, mixing of microfluidic, etc. are other applications of microvalves. In addition, microvalves are also used in medical applications. For example, they are used in the treatment of hydrocephalus. This system is in the brain and causes the diversion of cerebrospinal fluid and may relieve symptoms.

There are a variety of NMP valve designs. Lee et al . presented techniques for design and testing of fixed microvalves including the Tesla-type and the diffuser valve. The simplest configuration is shown in Figure 1, which is roughly like that designed in the macro-scale by Tesla. It has a bifurcated channel that re-enters the main flow channel perpendicularly when the flow is in the reverse direction. In the forward direction, most of the flow is carried by the main channel with reduced pressure losses.

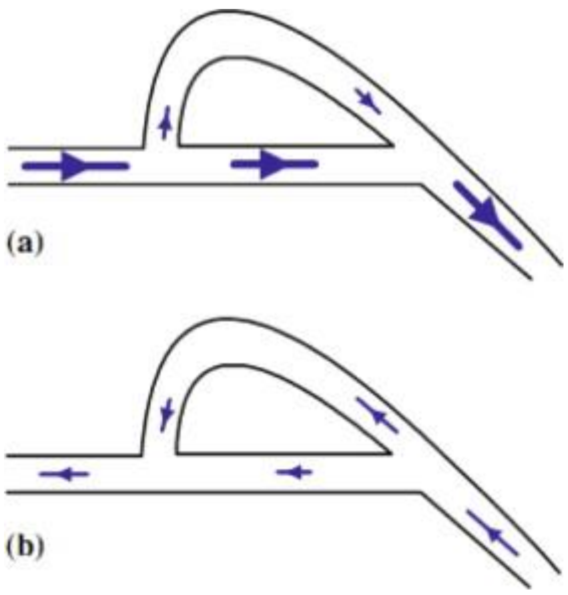

Figure 1. Tesla microvalve; a) in the forward direction, b) in the reverse direction

3. Flow geometry:

The geometry of Tesla microvalve is shown in Figure 2. It is consisted of six regions: 1) inlet channel, 2) main channel, 3) side-channel, 4) T-junction, 5) Y-junction and 6) outlet channel

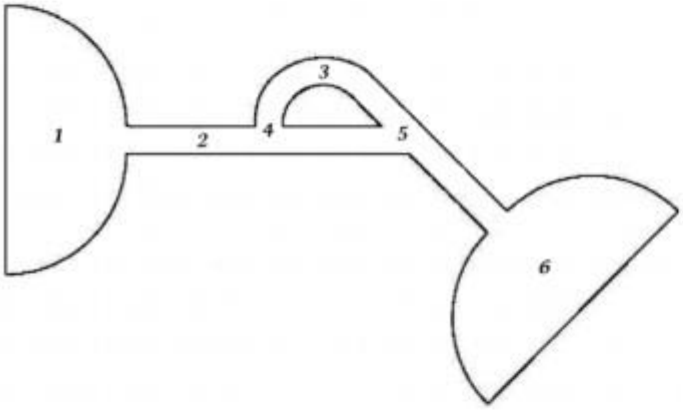

Figure 2. Geometry of the Tesla microvalve

The ability of a microvalve to pass flow in the forward direction while inhibiting flow in the reverse direction is the diodicity of the valve. Since NMP valves have more resistance to flow in the reverse direction than in the forward direction, they produce a unidirectional net flow in the downstream direction even in the presence of a backpressure. The remaining portion of the instantaneous flow is the oscillatory slosh flow. In an electrical analogy, the instantaneous current is a sum of an alternating current (slosh flow) and a direct current (net flow).

4. Numerical simulation

In inlet boundary, velocity is assumed to be constant and pressure is extrapolated from the field. At outlet boundary, the static pressure is assumed to be constant and other flow parameters such as velocity and temperature are determined by interpolation. No-slip condition is applied on the walls. In this simulation, because of cavitation limitations, we limited the pressure difference to $\Delta P < 1$ atm. The reverse flow calculation is done with $\Delta P = 0.1, 0.5, 0.9$ atm. Mass flow passing through the microvalve with this pressure difference is recorded. Then, average pressure P¯Inlet is measured in inlet boundary and ΔPForward is calculated through ΔPForward=P¯Inlet−POutlet. These values are used in Eq. (1) and the diodicity is calculated. The computational fluid dynamic software FLUENT is implemented for simulation of three different Tesla microvalve. They include T45A, T45C and T45CDeep made by Stanford Nanofabrication Facility. Cooper type Hex/Wedge element is used to mesh the model as shown in Figure 3. The number of produced elements for T45A, T45C and T45CDeep is 324562, 379470 and 475592, respectively.

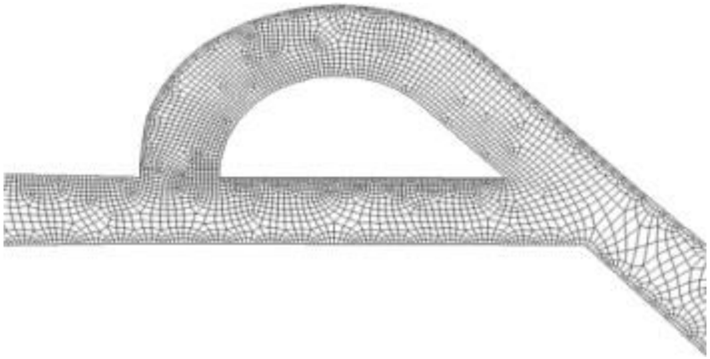

Figure 3. Mesh of T45A microvalve

5. Results and Discussion

a. Diodicity mechanism of T45A

Velocity field at symmetric plane is shown in Figure 4 and Figure 5 for forward and reverse flows with Re = 528, respectively. It is obvious that the velocity field is severely different for forward and reverse flows. In the case of forward flow, the fluid is accelerated at the entrance of fluid from goblet-shaped plenum to the channel and velocity gradient is created. While, the flow is developing, it reaches into the T-junction. Some of the flow is drawn into the side-channel and a small jet is formed along the guide vane in the side-channel. However, about 85% of the main channel fully developed flow continues to its route without any disturbance (Figure 6). At this stage, as much as Tesla valve has ability to pass much more volume through the main channel, the diodicity will be higher.

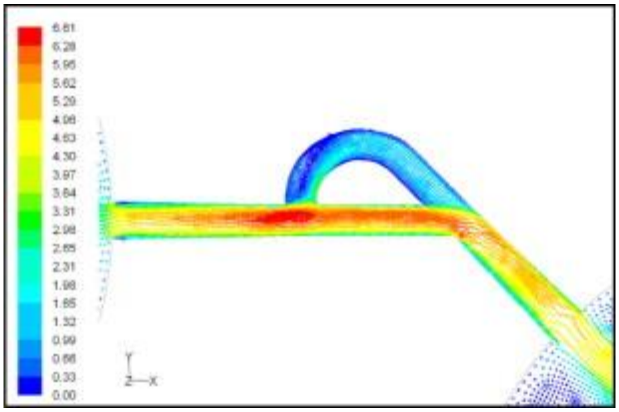

Figure 4. The forward flow velocity filed at symmetric plane for T45A with Re=528 based on hydraulic diameter of the cannel

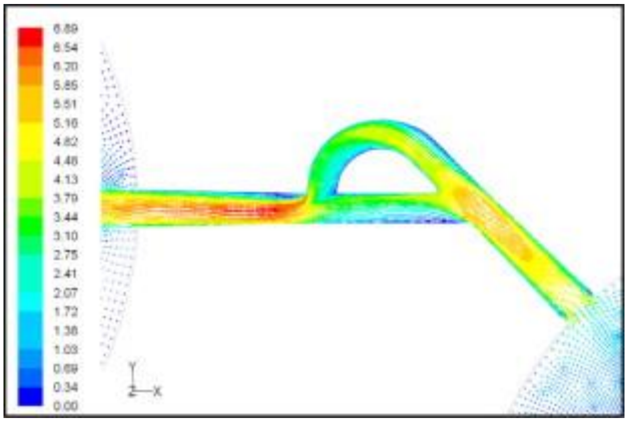

Figure 5. The reverse flow velocity filed at symmetric plane for T45A with Re=528 based on hydraulic diameter of the channel

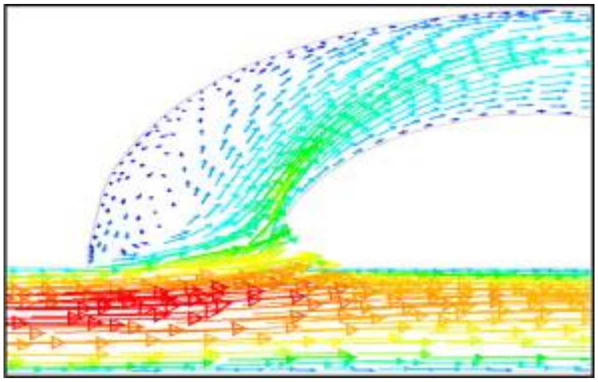

Figure 6. Jet formation at side-channel

The side-channel jet is expanded to the goblet section of the channel as a low-speed flow (as it gains 20% of the main channel maximum speed) and reaches to the Y-junction. However, it has enough momentum to divert the main channel flow before its reaching to the upper wall of Y-junction. It causes the diodicity improvement (Figure 7). The flow separation occurs at lower wall of Y-junction downstream and narrow jet of high velocity is formed near the upper wall (Figure 7). High velocity gradient between the jet and the wall causes additional losses and reduction in diodicity. Most parts of the channel are filled with low-speed areas, which narrowing these areas may be increase diodicity . Finally, the flow is exited from the output channel and enters the goblet-shaped plenum.

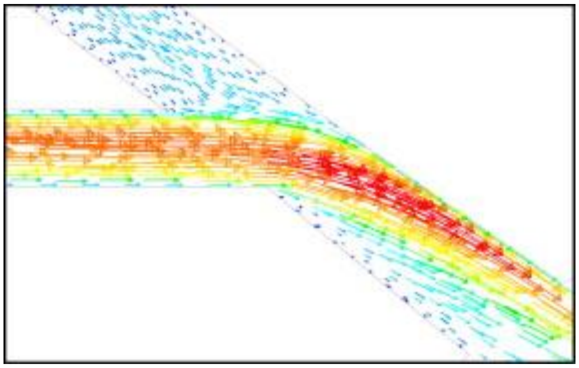

Figure 7. The diversion of mainstream by secondary jet stream during the direct flow

b. Diodicity mechanism of T45C

The difference between T45C and T45A is the angle of main and side channel at T-junction. The angle is higher for T45A and the length of channel is lower. Velocity and pressure fields at symmetric plane are shown in Figure 13 and Figure 14 for forward flow with Re = 519, respectively.

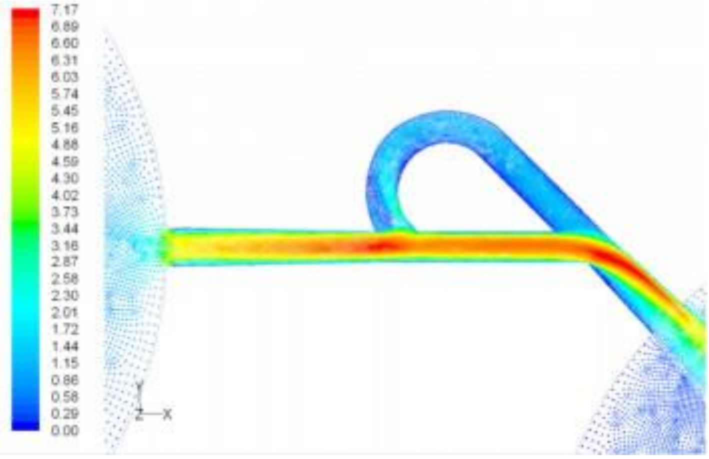

Figure 13. The forward flow velocity filed at symmetric plane for T45C with Re=519 based on hydraulic diameter of the channel

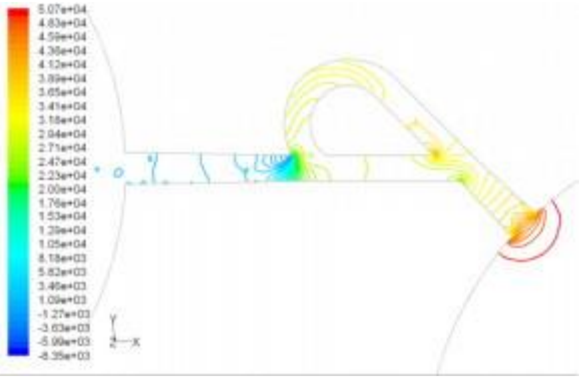

Figure 14. The forward flow pressure filed at symmetric plane for T45C with Re=519 based on hydraulic diameter of the channel

In this model, due to variation in the angle between side and main channels, a higher amount of flow rate passes through the main channel in forward flow. Velocity and pressure fields at symmetric plane are shown in Figure 15 and Figure 16 for reverse flow with Re = 519, respectively. Table 2 shows the values of diodicity for T45C microvalve at different conditions.

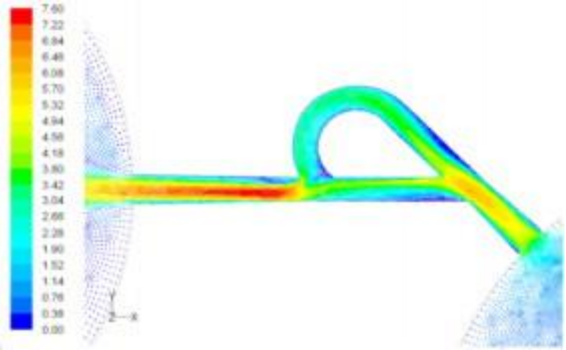

Figure 15. The reverse flow velocity filed at symmetric plane for T45C with Re=519 based on hydraulic diameter of the channel

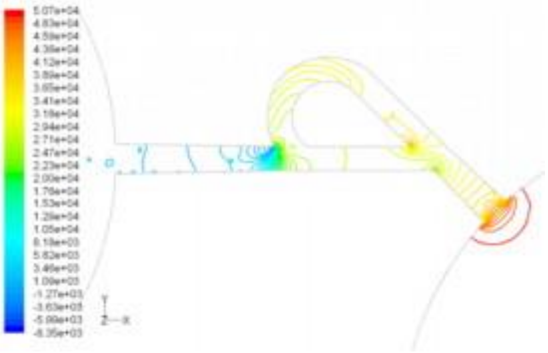

Figure 16. The reverse flow pressure filed at symmetric plane for T45C with Re=519 based on hydraulic diameter of the channel

6. Conclusions

In this paper, diodicity mechanism is investigated in a side-channel and T-junction of different Tesla-type microvalves by using FLUENT CFD package. Other parts of the valve have slight diodicity effect and result in slight increase in overall valve diodicity. If there is no need to inlet and outlet flow channels, the overall diodicity can be increased up to 2. Velocity field show that in forward flow a jet is formed in outlet channel and one is formed in inlet channel in reverse flow, but, the laminar jet of direct flow is weaker and is at the downstream of the cusp, while the jet is stronger without cusp, therefore, the energy loss is more severe in the surrounding area. The pressure field indicated that pressure drop at Y-junction is much severe in reverse flow. If you consider a complete valve, about two-thirds of the pressure work is lost and only a third of it is converted to the energy flux, So, the viscosity effects overcome the inertia effects at low Reynolds number in these microvalves. Furthermore, by increasing the number of valves and pressure difference, diodicity increases.

7. References:

Bae, Byunghoon, Nakhoon Kim, Hongseok Kee, Seon-Ho Kim, Yeon Lee, Sangho Lee, and Kyihwan Park. "Feasibility Test of an Electromagnetically Driven Valve Actuator for Glaucoma Treatment." *Journal of Microelectromechanical Systems* 11, no. 4 (2002): 344-54.

Kim, Ki-Won, Pyeong-Seok Cho, Sun-Jung Kim, Jong-Heun Lee, Chong-Yun Kang, Jin-Sang Kim, and Seok-Jin Yoon. "The Selective Detection of C 2 H 5 Oh Using Sno 2–Zno Thin Film Gas Sensors Prepared by Combinatorial Solution Deposition." *Sensors and Actuators B: Chemical* 123, no. 1 (2007): 318-24.

Lee, Gwo-Bin, Tzu-Ying Kuo, and Wan-Yu Wu. "A Novel Micromachined Flow Sensor Using Periodic Flapping Motion of a Planar Jet Impinging on a V-Shaped Plate." *Experimental Thermal and Fluid Science* 26, no. 5 (2002): 435-44.

Li, HQ, DC Roberts, JL Steyn, KT Turner, O Yaglioglu, NW Hagood, SM Spearing, and MA Schmidt. "Fabrication of a High Frequency Piezoelectric Microvalve." *Sensors and Actuators A: Physical* 111, no. 1 (2004): 51-56.

Morganti, E, and G Pignatel. "Microfluidics for the Treatment of the Hydrocephalus." Paper presented at the Proceedings of International Conference on Sensing Technology, Palmerston North, 2005.

Morris, Christopher J, Jone Y Chung, Patricia E Rahm, Fred K Forster, Dan Faulkner, and Reza Shekarriz. "Electronic Cooling Systems Based on Fixed-Valve Micropump Networks." Paper presented at the Solid-State Sensor, Actuator and Microsystems Workshop, Transducers Research Foundation, Inc, 2004.

Morris, Christopher J, and Fred K Forster. "Low-Order Modeling of Resonance for Fixed-Valve Micropumps Based on First Principles." *Journal of Microelectromechanical Systems* 12, no. 3 (2003): 325-34.

Nobakht, A. Y., M. Shahsavan, and A. Paykani. "Numerical Study of Diodicity Mechanism in Different Tesla-Type Microvalves." *Journal of Applied Research and Technology* 11, no. 6 (2013): 876-85.

Nobakht, Ali Yousefzadi, and R. Khoshbakhi Saray. "Using Genetic Algorithm and Multi Zone Combustion Model for Optimization of Gri- Mech 3.0 Mechanism in Hcci Engines." Paper presented at the The Third Fuel & Combustion Conference Of Iran, 2010.

Pal, Rohit, Ming Yang, Brian N Johnson, David T Burke, and Mark A Burns. "Phase Change Microvalve for Integrated Devices." *Analytical chemistry* 76, no. 13 (2004): 3740-48.

Rich, Collin A, and Kensall D Wise. "A High-Flow Thermopneumatic Microvalve with Improved Efficiency and Integrated State Sensing." *Journal of Microelectromechanical Systems* 12, no. 2 (2003): 201-08.

Singhal, Vishal, Suresh V Garimella, and Jayathi Y Murthy. "Low Reynolds Number Flow through Nozzle-Diffuser Elements in Valveless Micropumps." *Sensors and Actuators A: Physical* 113, no. 2 (2004): 226-35.

Suzuki, Hiroaki, and Rei Yoneyama. "Integrated Microfluidic System with Electrochemically Actuated on-Chip Pumps and Valves." *Sensors and Actuators B: Chemical* 96, no. 1 (2003): 38-45.

Yang, Xue'en, Alexander Holke, Stuart A Jacobson, Jeffrey H Lang, Martin A Schmidt, and Stephen D Umans. "An Electrostatic, on/Off Microvalve Designed for Gas Fuel Delivery for the Mit Microengine." *Journal of Microelectromechanical Systems* 13, no. 4 (2004): 660-68.

Yousefzadi Nobakht, Ali. "Study of Diodicity Mechanism in Different Tesla-Type Microvalves and Effect of Valve Arrangement on Effective Diodicity Parameter." Urmia University, 2007.

Yousefzadi Nobakht, Ali, and Hamidreza Mahabadipour. "Cfd Simulation of Tesla-Type Microvalves." Paper presented at the 13TH Conference of the Iranian society of Mechanical Engineers (ISME13), 2005.